Journal of the Korean Society for Nondestructive Testing
Vol. 23, No. 6 (2003. 12)

A Study for the Measurement of a Fluid Density in a Pipe Using Elastic Waves

Jin Oh Kim*,†, Kyo Kwang Hwang* and Haim H. Bau**

Abstract The effect of liquid confined in a pipe on elastic waves propagating in the pipe wall was studied theoretically and experimentally. The axisymmetric motion of the wave was modeled with the cylindrical membrane shell theory. The liquid pressure satisfying the axisymmetric wave equation was included in the governing equation as a radial load. The phase speed of the wave propagating in the axial direction was calculated, accounting for the apparent mass of the liquid. Experiments were performed in a pipe equipped with ring-shaped, piezoelectric transducers that were used for transmitting and receiving axisymmetric elastic waves in the pipe wall. The measured wave speeds were compared with the analytical ones. This work demonstrates the feasibility of using pipe waves for the determination of the density and, eventually, the flow rate of the liquid in a pipe.

Keywords: elastic waves, densimetry, fluid-structure interaction, phase speed, piezoelectric transducer

1. Introduction

Ultrasonics provides a convenient, non-intrusive means for the measurement of various properties of liquids confined in pipes and tanks (Lynnworth, 1989). The ultrasonic transducers can be mounted on the pipe or container's outer walls and can be maintained and replaced without any downtime.

The conventional design of an ultrasonic flowmeter was depicted schematically in Fig. 1(a). In this scheme, one measures the time-of-flight of an ultrasonic wave propagating between a transmitter and a receiver (Busch-Vishniac, 1999). In this method, however, as the tube's diameter decreases so does the measurement sensitivity. Moreover, it may be difficult to design sufficiently small transducers for small diameter tubes.

In order to overcome some of the disadvantages of conventional ultrasonic flowmeters, this paper suggests the use of annular transmitters as shown in Fig. 1(b). The cylindrical transducers (Kim et al., 2003) generate and detect axisymmetric waves that are transmitted in the pipe wall. One transducer excites radially the pipe and induces an axisymmetric wave that propagates along the pipe wall. A second transducer detects the wave at some distance from the point of origin, and the propagation time is measured. This propagation time is affected by the characteristics of the fluid confined in the pipe.

The effect of fluids on elastic waves propagating in solid pipes is one example of fluid-structure interaction problems (Junger and Feit, 1986; Grighton, 1988). The wave motion in a pipe without fluid loading has been extensively

Received: October 2, 2003. Accepted: November 21, 2003. * Dept. of Mechanical Engineering, Soongsil University, 1 Sangdo-dong, Dongjak-gu, Seoul, 156-743 Korea ** Dept. of Mechanical Engineering and Applied Mechanics, University of Pennsylvania, U.S.A. † Corresponding author: jokim@ssu.ac.kr

studied by utilizing the full equations of elasticity (Gazis, 1959) and by using thin shell theory (Graff, 1991). A considerable amount of work has also been done on fluid-loaded shells (Brevart and Fuller, 1993).

This paper presents the feasibility of measuring fluid density in a pipe using elastic waves as a first step towards the design of an ultrasonic flowmeter of the type depicted in Fig. 1(b). The paper was organized as follows. Section 2 described the mathematical model for elastic waves propagating in the thin walls of pipes containing liquids. In section 3, dispersion equations relating the wave speed to the frequency were derived. Section 4 described the experimental set-up and measurements. These measurements were subsequently compared with experimental observations. Section 5 summarized the results and made a conclusion.

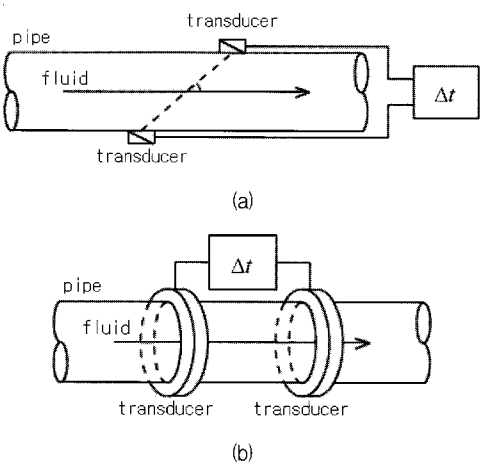

Fig. 1 Schematic diagram of ultrasonic flowmeters of the conventional type (a) and of the new design (b)

2. Mathematical Model

Consider elastic waves propagating in a pipe having an inner radius R and wall thickness h. Figure 2 depicts a segment of the pipe's wall. We have treated the pipe wall as a thin shell. Shell theory has the advantage of providing simpler expressions than the ones generated using the full equations of linear elasticity. The theory is known to yield reasonable results as long as $h/R \ll 1$ and the wavelengths are large compared to the wall thickness ($kh \ll 1$). In the above, k is the wavenumber.

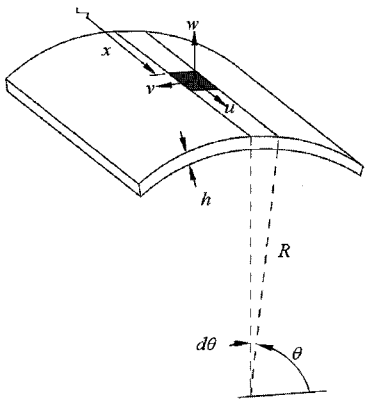

Fig. 2 Coordinates and displacement components in an element of a cylindrical shell

The major approximations in the analysis were:

(1) The pipe is perfectly circular, concentric, and infinitely long.
(2) The liquid in the pipe is ideal, i.e. inviscid, compressible, irrotational, and stationary.
(3) Transverse shear stresses and bending and twisting moments are neglected, and all stresses are averaged across the thickness of the pipe to eliminate any radial dependence.
(4) The pipe is not pre-stressed, i.e. static stresses due to liquid pressure, pipe weight, and mounting are neglected, and all stresses in the pipe are the result of the induction of the elastic waves.

In the special case of an axisymmetric, cylindrical membrane shell, the general thin shell theory (Junger and Feit, 1986) simplifies to

$$\frac{\partial^2 u}{\partial x^2} + \frac{\nu}{R}\frac{\partial w}{\partial x} = \frac{1}{c_p^{\,2}}\frac{\partial^2 u}{\partial t^2} \tag{1}$$

and

$$-\frac{w}{R^2} - \frac{\nu}{R}\frac{\partial u}{\partial x} + \frac{q}{\rho_s h\, c_p^{\,2}} = \frac{1}{c_p^{\,2}}\frac{\partial^2 w}{\partial t^2} \tag{2}$$

In the above $u(x,t)$ and $w(x,t)$ are, respectively, the axial and radial displacements; x is the axial coordinate; t is time; q is the radial load;

$$c_p = \sqrt{E/\rho_s(1-\nu^2)} \tag{3}$$

is the longitudinal 'thin-plate' velocity; E is the Young's modulus; ρ_s is the solid's density; and ν is Poisson's ratio of the pipe material.

The liquid pressure p satisfies the wave equation (Kinsler et al., 2000)

$$\frac{\partial^2 p}{\partial r^2} + \frac{1}{r}\frac{\partial p}{\partial r} + \frac{\partial^2 p}{\partial x^2} = \frac{1}{c_l^2}\frac{\partial^2 p}{\partial t^2} \tag{4}$$

where c_l is the sound speed in the liquid medium. The radial pressure q in eqn. (2) equals the pressure p at $r = R$, i.e.

$$q = p\,|_{r=R} \tag{5}$$

Once the pressure equation is solved, the radial liquid velocity v_r can be computed using the linearized radial momentum equation:

$$\frac{\partial v_r}{\partial t} = -\frac{1}{\rho_l}\frac{\partial p}{\partial r} \tag{6}$$

At the pipe surface

$$\left.\frac{\partial v_r}{\partial t}\right|_{r=R} = \frac{\partial^2 w}{\partial t^2} \tag{7}$$

Equations (6) and (7) are combined to obtain the relation between w and p:

$$\left.\frac{\partial p}{\partial r}\right|_{r=R} = -\rho_l \frac{\partial^2 w}{\partial t^2} \tag{8}$$

We seek solutions for the wave propagation of the form

$$u(x,t) = U\, e^{ik(x-ct)}, \tag{9a}$$

$$w(x,t) = W\, e^{ik(x-ct)}, \tag{9b}$$

$$p(x,r,t) = P(r)\, e^{ik(x-ct)}, \tag{9c}$$

where c is the phase speed of the wave in the pipe wall.

Upon substituting eqn. (9c) in eqn. (4), a modified Bessel equation is obtained for the pressure amplitude $P(r)$.

$$\frac{d^2P}{dr^2} + \frac{1}{r}\frac{dP}{dr} - k^2\left(1 - \frac{c^2}{c_l^2}\right)P = 0 \tag{10}$$

In general, the axial wavenumber k can be complex, and the imaginary part represents the attenuation. In this work, k is assumed to be real, and $k = \omega/c$, where ω is the circular frequency of the wave.

Equation (10) admits a solution of the form:

$$P(r) = A\, I_0(\gamma r) + B\, K_0(\gamma r) \tag{11}$$

where γ is the radial wavenumber expressed as:

$$\gamma = k\sqrt{1 - \left(\frac{c}{c_l}\right)^2} = \frac{\omega}{c}\sqrt{1 - \left(\frac{c}{c_l}\right)^2} \tag{12}$$

Witness that $\gamma = \gamma(c,k)$ or $\gamma = \gamma(c,\omega)$. When $c < c_l$, γ is real. When $c > c_l$, γ is imaginary. The cut-off frequency $\omega_c = k\, c_l$. In eqn. (11) I_0 and K_0 are modified Bessel functions of the first kind and of order 0. $I_0(0)$ is finite while $K_0(0)$ is infinite. Thus, to assure bounded solutions at $r = 0$, B is set to 0.

Since

$$\left.\frac{dP}{dr}\right|_{r=R} = A\left.\frac{dI_0(\gamma r)}{dr}\right|_{r=R} = A\,\gamma\, I_1(\gamma R) \tag{13}$$

the boundary condition (8) can be rewritten as

$$\begin{aligned} p\,|_{r=R} &= A\, I_0(\gamma R)\cdot e^{i(kx-\omega t)} \\ &= -\rho_l \frac{I_0(\gamma R)}{\gamma\, I_1(\gamma R)}\cdot \end{aligned} \tag{14}$$

Equation (14) includes the apparent mass of the liquid per unit area:

$$M(\gamma) = \rho_l \frac{I_0(\gamma R)}{\gamma\, I_1(\gamma R)} \tag{15}$$

Upon expressing the liquid pressure in terms of the radial displacement of the wall, eqn. (2) can be rewritten as

$$-\frac{w}{R^2} - \frac{\nu}{R}\frac{\partial u}{\partial x} = \left(1 + \frac{M(\gamma)}{\rho_s h}\right)\frac{1}{c_p^2}\frac{\partial^2 w}{\partial t^2} \tag{16}$$

The above expression suggested that the effect of the liquid would increase as the radial wavenumber γ increased and the solid density ρ_s, and the shell thickness h decreased.

3. Dispersion Relations

Upon substituting eqns. (9a) and (9b) into eqns. (1) and (16), one obtains

$$k^2\left[1-\left(\frac{c}{c_p}\right)^2\right]U - ik\frac{\nu}{R}W = 0 \tag{17}$$

and

$$ik\frac{\nu}{R}U + \left[\frac{1}{R^2} - \left(1+\frac{M(\gamma)}{\rho_s h}\right)k^2\left(\frac{c}{c_p}\right)^2\right]W = 0 \tag{18}$$

Requiring that the equations admit non-trivial solutions and introducing the dimensionless quantities

$$\bar{c}=\frac{c}{c_p},\ \bar{k}=kh,\ \bar{h}=\frac{h}{R},\ \text{and}\ \bar{M}(\bar{\gamma})=\frac{M(\gamma)}{\rho_s h} \tag{19}$$

one obtains the characteristic equation:

$$\left(1+\bar{M}\right)\left(\frac{\bar{k}}{\bar{h}}\right)^2\bar{c}^{-4} - \left[1+\left(1+\bar{M}\right)\left(\frac{\bar{k}}{\bar{h}}\right)^2\right]\bar{c}^{-2} + \left(1-\nu^2\right) = 0 \tag{20}$$

Equation (20) represents the dispersion relation between the non-dimensional phase speed $\bar{c}$ and the non-dimensional wavenumber $\bar{k}$.

The equation can be expressed in terms of the dimensionless frequency

$$\bar{\omega}=\frac{\omega}{c_p/h}=\bar{k}\bar{c} \tag{21}$$

Eliminating $\bar{k}$ from eqn (20) produces the relation between $\bar{c}$ and the dimensionless frequency $\bar{\omega}$:

$$1-\nu^2-\left(1+\bar{M}\right)\left(\frac{\bar{\omega}}{\bar{h}}\right)^2 - \left[1-\left(1+\bar{M}\right)\left(\frac{\bar{\omega}}{\bar{h}}\right)^2\right]\bar{c}^{-2} = 0 \tag{22}$$

3.1. A Pipe in Vacuum

When the pipe is in vacuum (or in air), $\bar{M} = 0$ and eqns (20) and (22) can be solved explicitly to obtain the phase speed ($\bar{c}$) as a function of the wavenumber,

$$\bar{c}^{-2}=\frac{\left[\left(\bar{k}/\bar{h}\right)^2+1\right]\pm\sqrt{\left[\left(\bar{k}/\bar{h}\right)^2-1\right]^2+4\nu^2\left(\bar{k}/\bar{h}\right)^2}}{2\left(\bar{k}/\bar{h}\right)^2} \tag{23}$$

and the frequency,

$$\bar{c}=\sqrt{\frac{1-\nu^2-\left(\bar{\omega}/\bar{h}\right)^2}{1-\left(\bar{\omega}/\bar{h}\right)^2}} \tag{24}$$

Figures 3(a) and 3(b) depict, respectively, the dimensionless phase speed $\bar{c}$ as a function of the dimensionless wavenumber $\bar{k}$ and the dimensionless phase speed $\bar{c}$ as a function of the dimensionless frequency $\bar{\omega}$. In both cases, $\nu = 0.3$. Since $d\bar{c}/d\bar{k} < 0$ in Fig. 3(a) and $d\bar{c}/d\bar{\omega} < 0$ in Fig. 3(b), the phase velocity is smaller than the group velocity.

When the frequency is high or the wall is thin ($\bar{\omega}/\bar{h} \gg 1$), $\bar{c}$ approaches 1 and the phase speed c approaches c_p, the speed of the longitudinal wave in a thin plate. Equation (17) implies that in this case $W = 0$ and the pipe has no motion in the radial direction. It is anticipated that in this case, there will be weak interaction between the waves propagating in the pipe wall and the confined liquid.

When the wave frequency is small and the pipe wall is thick ($\bar{\omega}/\bar{h} \gg 1$), $\bar{c}$ approaches $(1-\nu^2)^{1/2}$ and the phase speed c approaches the speed of the longitudinal wave in a rod $(E/\rho_s)^{1/2}$. Since the thin shell theory is used under the assumption of $\bar{h} \ll 1$, this case must correspond to very low frequencies.

When $\bar{\omega}/\bar{h}=1$, eqn. (18) implies $U = 0$ and there is no motion in the axial direction. This represents the cut-off frequency of the wave propagation.

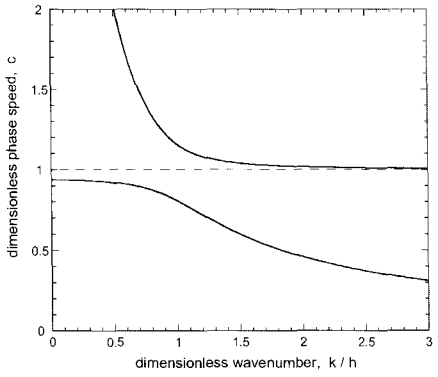

(a)

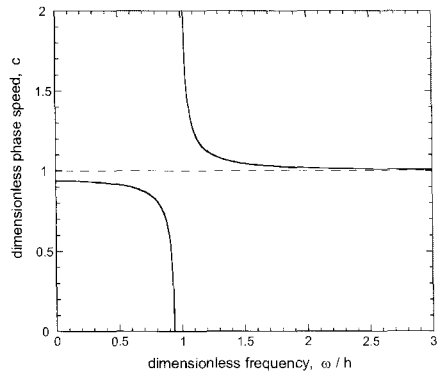

(b)

Fig. 3 Dispersion curves for an empty pipe. (a) the dimensionless phase speed as a function of the dimensionless wavenumber, (b) the dimensionless phase speed as a function of the dimensionless frequency.

3.2. Pipes with Confined Liquid

In the presence of liquid, the situation is considerably more complicated since $\bar{M}$ (eqns. 20 and 22) is a complicated function of $\bar{c}$.

3.2.1. When $c < c_l$

The radial wavenumber $\bar{\gamma}$ (eqn. 12) is real when $c < c_l$, and there are no pressure oscillations in the radial direction. The dimensionless apparent mass of the liquid is:

$$\bar{M}(\bar{\gamma}) = \bar{\rho}\,\frac{I_0(\bar{\gamma}/\bar{h})}{\bar{\gamma}\, I_1(\bar{\gamma}/\bar{h})} \tag{25}$$

where $\bar{\gamma}=\gamma h$ and $\bar{\rho}=\rho_l/\rho_s$. Figure 4(a) depicts $\bar{M}(\bar{\gamma})$ as a function of $\bar{\gamma}$. In the limiting case of long wavelengths $(\bar{\gamma}\to 0)$, the dimensionless apparent mass $\bar{M}(\bar{\gamma})\to 2\bar{\rho}/\bar{\gamma}^2$. In the other extreme of short wavelengths $(\bar{\gamma}\to\infty)$, the dimensionless apparent mass $\bar{M}(\bar{\gamma})\to\bar{\rho}/\bar{\gamma}$.

3.2.2. When $c > c_l$

When $c > c_l$, the radial wavenumber $\bar{\gamma}$ is imaginary. In this case, we substitute $\bar{\eta}=i\,\bar{\gamma}$ and replace the modified Bessel functions in eqn (11) with regular Bessel functions. The dimensionless form of the apparent liquid mass is:

$$\bar{M}(\bar{\eta}) = \bar{\rho}\,\frac{J_0(\bar{\eta}/\bar{h})}{\bar{\eta}\, J_1(\bar{\eta}/\bar{h})} \tag{26}$$

The Bessel functions of the first kind, $J_n(x)$, are oscillatory functions of x. Thus $\bar{M}$ varies from $-\infty$ to $+\infty$ somewhat like $\cot(\eta)$. This behavior is depicted in Fig. 4(b).

3.2.3. Dispersion Curves

Equations (20) and (22) were solved numerically to obtain the dispersion relations. Fig. 5(a) and 5(b) depict, respectively, the dimensionless phase speed $\bar{c}$ as a function of the wavenumber $\bar{k}/\bar{h}$ and $\bar{c}$ as a function of the frequency $\bar{\omega}/\bar{h}$. In contrast to the case of the empty pipe (Fig. 3), Fig. 5 exhibits a large number of modes. The various modes are labeled with Roman numerals. The presence of a large number of modes could have been anticipated based on the large number of branches of the apparent liquid mass (Fig. 4b).

The curve I in Figs. 5(a) and 5(b) represents the dimensionless phase speed of the wave in the liquid rather than in the pipe wall. Similar to the curves in Fig. 3(b) for an empty pipe, the dispersion curves in Fig. 5(b) exhibit sudden drops.

The curves II, III, IV, etc. represent the waves in the pipe shell that are affected by the liquid's presence. The curve II, which corresponds to the fundamental mode, has a zero slope at both low and high frequencies. The dispersion curves of this mode for the empty pipe and for the filled pipe are compared in Fig. 6, which shows clearly the effect of the liquid on the phase speed of the wave. When the frequency is low and the shell wall is relatively thick $(\bar{\omega}/\bar{h} << 1)$, the dimensionless fundamental mode's phase speed $\bar{c}$ approaches $(1-\nu^2)^{1/2}$, which is the wave speed in an empty pipe. As $\bar{\omega}/\bar{h}$ is larger, the curve approaches the phase speed of the wave in the liquid.

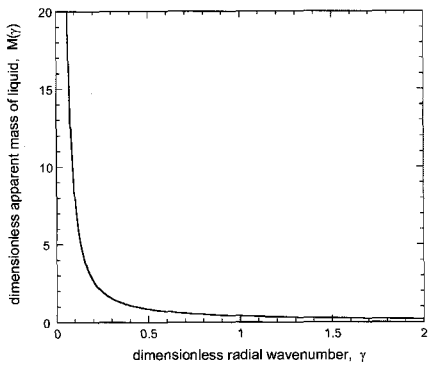

(a)

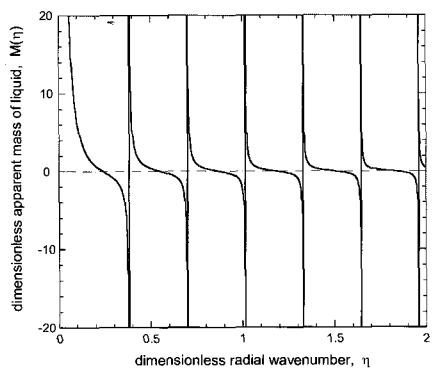

(b)

Fig. 4 The apparent mass as a function of the radial wavenumber when $c < c_l$ (a) and when $c > c_l$ (b)

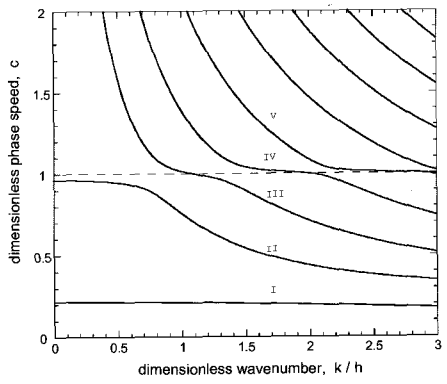

(a)

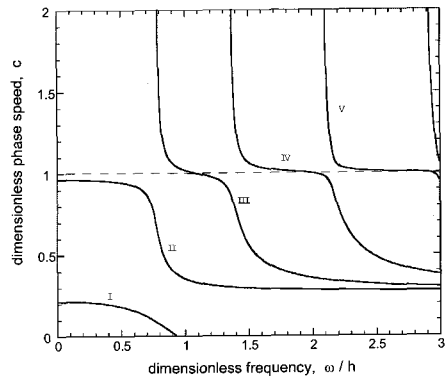

(b)

Fig. 5 Dispersion curves for a pipe containing stationary water. (a) the dimensionless phase speed as a function of the dimensionless wavenumber, (b) the dimensionless phase speed a a function of the dimensionless frequency

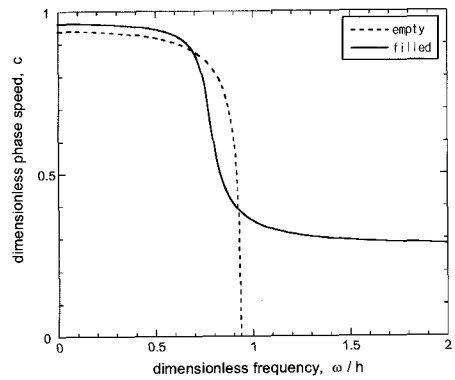

Fig. 6 Dispersion curves of the fundamental mode for the empty pipe and for the liquid-filled pipe

The curves III, IV, V, etc., which correspond to the higher modes, exhibit common behavior. In an intermediate range of $\bar{\omega}/\bar{h}$, the curves have flat regions with $\bar{c}$ equal to 1, which represents the phase speed of the longitudinal wave in a thin plate. This corresponds to the case of $W = 0$ in eqn. (17), i.e., the case of no radial motion. When $(\bar{\omega}/\bar{h} << 1)$, the curves approach the phase speed of the wave in the liquid.

4. Experiment

In the previous section, the effect of a liquid confined in a pipe on the elastic waves propagating in the pipe wall was analyzed theoretically. Based on the theoretical analysis, it is anticipated that by measuring the wave's speed, it should be possible to deduce the liquid's mass density. The objective of this section is to demonstrate that the trends predicted by the theory can be duplicated in experiments.

4.1. Experimental Apparatus

Piezoelectric cylindrical transducers (Kim et al., 2003) were used to generate and detect the elastic waves in the pipe wall. Three pairs of semi-annular, cylindrical transducers (ISTec Inc.), were installed around an aluminum (1100-H14) pipe, whose outer radius was 8 mm, wall thickness was 1 mm, and whose length was 1200 mm, as depicted in Fig. 7(a). A photograph of one transducer is shown in Figure 7(b). Pairs of semi-annular cylindrical transducers can be easily installed on the outer face of a pipe in the similar way to a device used for bending wave sensing system (Liu and Lynnworth, 1995).

In Fig. 7(a), the transducer denoted *T* is the transmitter and the transducers denoted *R1* and *R2* are receivers. *R1* and *R2* were installed, respectively, distances L_1 and L_2 from the transmitter *T*. The distances L_1 and L_2 were much smaller than the total length of the pipe. Fig. 8 depicts schematically the experimental set-up. The set-up consisted of a function generator (Agilent 33120A), a power amplifier (Eliezer HA 400), and a digital oscilloscope (Tektronix TDS3032).

Electrical pulse signals produced by the signal generator and amplified by the power amplifier were sent to the transducer *T*. The transmitting transducer *T* converted the electrical pulse into mechanical vibrations, which in turn induced radial waves that propagated along the pipe's wall. The receiving transducers R_1 and R_2 detected the elastic waves and converted the mechanical vibrations into electric signals. The transmitted and received signals were sent to the oscilloscope.

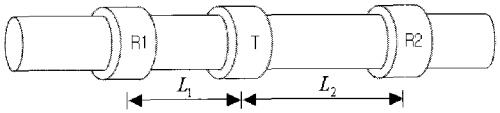

(a)

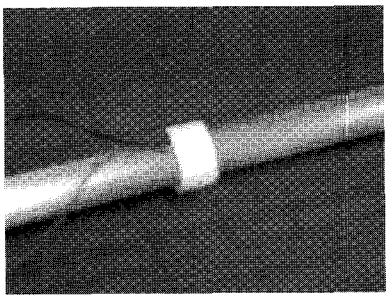

(b)

Fig. 7 The arrangement of transducers along a pipe. (a) the transmitter *T* and the two receivers *R1* and *R2*, (b) a photograph of a transducer installed around a pipe

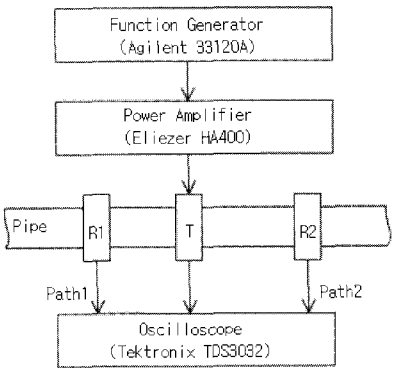

Fig. 8 Schematic diagram of the experimental set-up

We refer to the path of the wave propagation from T to $R1$ as Path 1 and the path from T to $R2$ as Path 2. Paths 1 and 2 had different lengths.

4.2. Experimental Results

First, experiments were performed in the empty pipe (without any liquid). These experiments were used to estimate the acoustic distances between the transmitter and the two receivers. Subsequently, experiments were carried out in a pipe filled with liquid. The measured values of the wave speed are compared with the calculated values.

4.2.1. For the Pipe without Liquid

The phase speed of the elastic wave propagating in the pipe wall was experimentally determined by dividing the distance between the transmitter and receiver with the time that elapsed between transmission and reception. The transducers, however, had a finite width in the propagation direction and the distance traveled by the wave was not well defined. To overcome this problem, we defined the effective distance by multiplying the measured time-of-flight by the known wave speed in an empty pipe,

$$c = c_p \cdot \bar{c}, \tag{27}$$

where $\bar{c}$ is given in eqn. (24). In the above, c_p is the phase speed of the longitudinal wave in a thin plate, and its value for aluminum 1100-H14 is 5,417 m/s (Beer and Johnston, 1995). The value of $\bar{\omega}$ needed for the calculation of c_p was obtained by analyzing the received signal. Figure 9 depicts an example of the frequency spectrum. The center frequency f is 76 kHz and $\omega(=2\pi f)$ is 477.5×10^3 rad/s. The value of the dimensionless frequency $\bar{\omega}$ is 0.0882 and $\bar{\omega}/\bar{h}$ = 0.663. Accordingly, $\bar{c}$ = 0.887, and the estimated phase speed c = 4806.5 m/s.

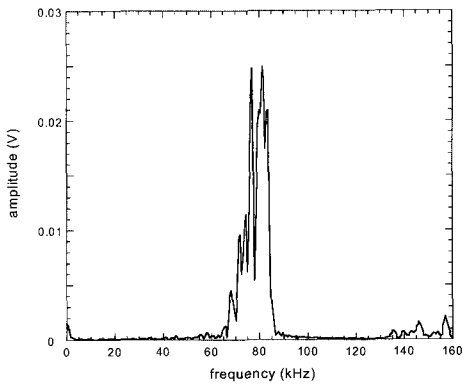

Fig. 9 The frequency spectrum of the received signal

Table 1 The dimensions of the pipe and the material properties of aluminum 1100-H14

	Items	Values
Pipe geometry	Mean radius, R	7.5 mm
	Thickness, h	1.0 mm
Material property	Mass density, ρ_s	2,710 kg/m^3
	Young's modulus, E	70 Gpa
	Shear modulus, G	26 Gpa
	Poisson's ratio, ν (= $E/2G - 1$)	0.346
Longitudinal wave speed in a plate, c_p (= $(E/\rho_s(1-\nu^2))^{1/2}$)		5,417 m/s

The transit time Δt was measured by monitoring the signals of the transmitting transducer T and the receiving transducers $R1$ and $R2$ as shown in Fig. 10. Figure 10(a) depicts the waveform of the pulse signal input to the transmitter T. Figs. 10(b) and 10(c) depict, respectively, the waveforms of the electric signals detected by the receivers $R1$ and $R2$. Witness that the pulse wave was dispersed during the propagation. The time lapses from the beginning of the original pulse in Fig. 10(a) to the beginning of the dispersed pulse in Figs. 10(b) and 10(c) are the transit times corresponding to the phase velocity. From the propagation speed c and the propagation time Δt, the effective distance is:

$$L = c \cdot \Delta t \tag{28}$$

Table 2 lists the transit time Δt, the theoretically calculated speed of the wave c, and the propagation distance $c \cdot \Delta t$ for Path 1 and Path 2. The distances between the two far ends of the transducers were 205 mm for Path 1 and 316 mm for Path 2, as listed in Table 2. The shortest distances were 181 mm for Path 1 and 292 mm for Path 2. The calculated distances, 200 mm for Path 1 and 310 mm for Path 2, fall between the shortest and largest distance between two adjacent transducers, and are close to the largest distance. The calculated distances L_1 and L_2 for Path 1 and Path 2, respectively, are used in the next section to measure the phase speed of the wave propagating in the pipe when it is filled with a liquid.

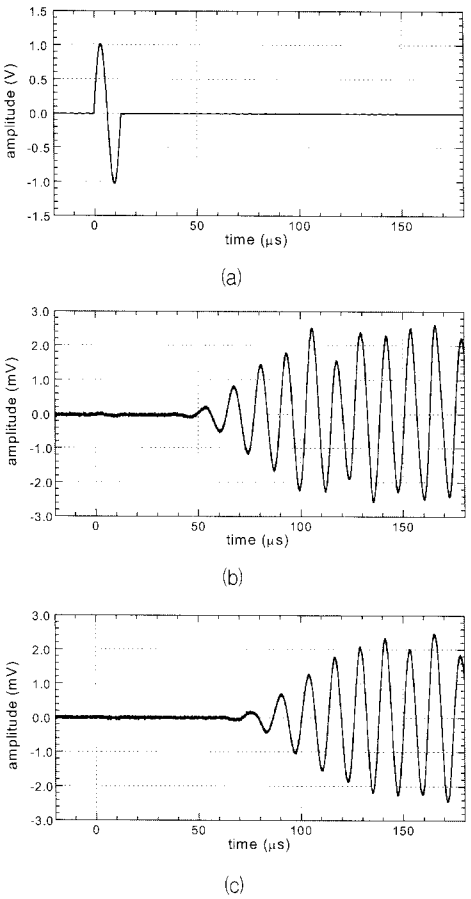

Fig. 10 The waveforms of the transmitted and received signals when the pipe is empty. (a) the transmitter *T*, (b) the receiver *R*1, (c) the receiver *R*2

Table 2 The measured propagation time and propagation distance of each path when the pipe is empty

Path	Propagation time Δt (μs)	Wave speed c (m/s)	Propagation distance (mm) $c \cdot \Delta t$	Maximum
1	41.7	4806.5	200	205
2	64.6	4806.5	310	316

4.2.2. Pipe Filled with Stationary Liquid

The pipe was filled with fresh water at temperature 20 ± 2℃. The mass density of the water (ρ_l) is 1,000 kg/m^3 and the phase speed of the wave in the water (c_l) is 1,481 m/s (Kinsler et al., 2000). The experimental procedure was the same as that in the empty pipe.

Fig. 11 depicts the signal's waveforms. The transit times Δt were measured between the start of the transmitted pulse in Fig. 11(a) and the beginning of the received signal in Fig. 11(b) or 11(c). Dividing the effective propagation distance L estimated in the previous section with the measured time Δt determines the phase speed of the wave in the liquid-filled pipe.

$$c = L/\Delta t \tag{29}$$

Table 3 Comparison between the measured and calculated wave speeds for each path when the pipe is filled with stationary water

Path	Measured time Δt (μs)	Propagation distance L (mm)	Wave speed (m/s) Measured	Wave speed (m/s) Calculated	Difference (%)
1	40.7	200	4,920.8	4,861.4	12.1
2	63.0	310	4,925.4	4,861.4	13.0

The measured values of the phase speed were summarized in Table 3 and compared with the theoretical values calculated with eqn. (22) and eqn. (27). The difference between the measured and calculated values is less than 13%.

Figure 12 compares the received signals in the case of the empty pipe (solid line) and the case of the liquid-filled pipe (dashed line). It appeared that the phase speed of the wave was faster in the liquid-filled pipe than in the empty pipe. This was consistent with the predictions of Fig. 6. When $\overline{\omega}/\overline{h} \sim 0.887$, the phase speed in the fluid-filled pipe was higher than in the empty pipe.

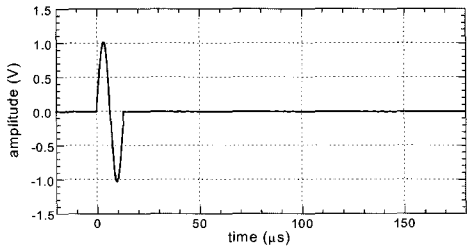

(a)

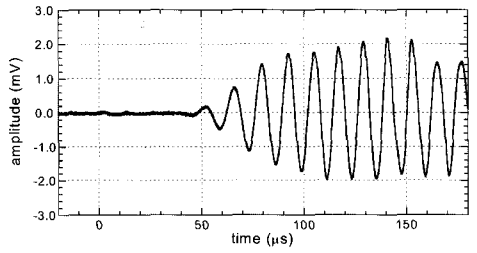

(b)

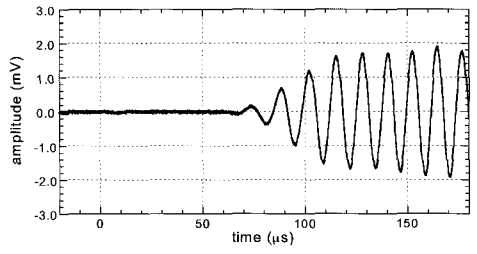

(c)

Fig. 11 The waveforms of the transmitted and received signals when the pipe is filled with water. (a) the transmitter T, (b) the receiver $R1$, (c) the receiver $R2$

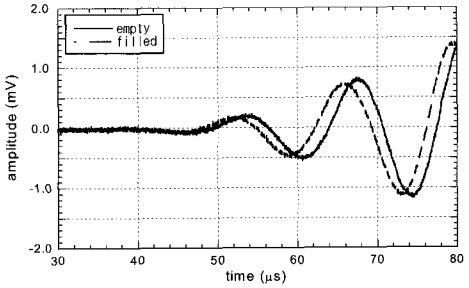

(a)

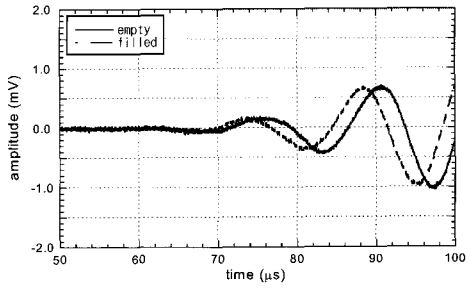

(b)

Fig. 12 Comparison of the received signals when the pipe is empty and when it is filled with stationary water. (a) Path 1 and (b) Path 2

5. Conclusion

The effect of a liquid confined in a pipe on the elastic waves propagating in the pipe wall has been studied theoretically and experimentally. The axisymmetric radial motion of the wave has been modeled by the cylindrical membrane shell theory taking into account the liquid pressure. The elastic equation in the solid and the Euler equation in the fluid were solved simultaneously to obtain the dispersion relations.

Experiments were performed using piezoelectric cylindrical transducers to transmit and receive axisymmetric elastic waves in the pipe wall. The measured wave speeds were compared and favorably agree with the calculated ones. The work presented in this paper demonstrates the feasibility of using the elastic waves for the measurement of the mass density of a liquid in a pipe.

Acknowledgment

The authors gratefully acknowledge useful discussions with Mr. L. C. Lynnworth of GE Panametrics.

References

Beer, F. P. and Johnson, Jr., E. R. (1995) *Mechanics of Materials*, 2nd ed., McGraw-Hill, Singapore

Brevart, B. J. and Fuller, C. R. (1993) Effect of an Internal Flow on the Distribution of Vibrational Energy in an Infinite Fluid-Filled Thin Cylindrical Elastic Shell, Journal of Sound and Vibration, Vol. 167, No. 1, pp. 149-163

Busch-Vishniac, I. J. (1999) *Electrome-chanical Sensors and Actuators*, Springer, New York, pp. 331-335

Crighton, D. G. (1989) Fluid Loading - The Interaction between Sound and Vibration, Journal of Sound and Vibration, Vol. 133, No. 1, pp. 1-27

Gazis, D. C. (1959) Three-Dimensional Investigation of the Propagation of Waves in Hollow Circular Cylinders, The Journal of the Acoustical Society of America, Vol. 31, No. 5, pp. 568-578

Graff, K. F. (1991) *Wave Motion in Elastic Solids*, Dover Publications, New York, pp. 258-266.

Junger, M. C. and Feit, E. (1986) *Sound, Structures, and Their Interaction*, 2nd edition, The MIT Press, Cambridge, pp. 215-218.

Kim, J. O., Hwang, K. K., and Jeong, H. G. (2004) Radial Vibration Characteristics of Piezoelectric Cylindrical Transducers, Journal of Sound and Vibration, in press

Kinsler, L. E., Frey, A. R., Coppens, A. V., and Sanders, J. V. (2000) *Fundamentals of Acoustics*, 4th ed., John Wiley & Sons, New York, pp. 133-135

Liu, Y. and Lynnworth, L. C. (1995) Elastic Wave Sensing System, United States Patent 5, 456, 114

Lynnworth, L. C. (1989) *Ultrasonic Measurements for Process Control*, Academic Press, Boston